

# Battery Management Maximum Power Point Tracking & Model Predictive Control and Voltage Regulation

Swetha.O<sup>1</sup>&Sri S.Maddileti <sup>2</sup>

<sup>1</sup>M-TECH, Dept. of EEE Geethanjali College of Engineering & Technology, Kurnool, AP

Mail: -[swethaonteddu5@gmail.com](mailto:swethaonteddu5@gmail.com)

<sup>2</sup> Assistant Professor Dept. of EEE Geethanjali College of Engineering & Technology, Kurnool, AP

Mail: - [maddiletysuddula@gmail.com](mailto:maddiletysuddula@gmail.com)

## Abstract

As the demand of Electricity is increasing day by day and is already more than the production of Electricity whereas reserves of fossil-fuel are depleting, there is a strong need to shift for other sources which are renewable energy sources. Regarding this, DC micro grids and their energy management of these renewable energy sources have gained more importance which is discussed in this paper. The main objective of the proposed system is to provide uninterrupted power supply to the load systems which are located at isolated sites of remote and rural areas. The proposed system mainly deals with implementation of Energy Management System (EMS) to DC microgrid using maximum power point tracking (MPPT) algorithm. A coordinated and multivariable EMS is proposed that employs a wind turbine and a photovoltaic array as controllable generators by adjusting the pitch angle and the switching duty cycles and a storage system consisting of batteries. In order to realize constant current, constant voltage (IU) charging regime and increase the life span of batteries, the proposed EMS require being more flexible with the power curtailment feature. The proposed strategy is developed as an online nonlinear model predictive control (NMPC) algorithm based on individual MPPTs of the system. The entire designed system is modeled and simulated using MATLAB/Simulink Environment.

**Keywords:**Battery Management, Maximum Power Point Tracking (MPPT), Nonlinear Model Predictive Control (NMPC), Power Sharing, and Voltage Regulation.

## 1. Introduction

The microgrid may operate as an extension of the main grid, (grid-connected) or as a standalone grid with no connection to the grid. Standalone dc microgrids have some distinct

applications automotive or marine industries, rural areas. Since ac systems suffer from the need of synchronization of several generators, dc microgrids are more efficient due to the fact that dc generators and storages do not need ac-

dc converters for being connected to dc microgrids. The few issues regarding voltage regulation, power sharing, and battery management, is severe in standalone green micro grids that consist of only intermittent solar and wind energy sources, and lead to the necessity of more controllable strategies. The grid voltage source converters are the primary slack terminals to regulate the voltage level of grid-connected microgrids. Battery banks, on the other hand, are effective slack terminals for standalone microgrids

Their energy absorbing capacities are limited regarding a number of operational constraints, as explained later in this section. In order to regulate the voltage level of standalone dc micro grids. Present load shedding strategies for the cases in which there is insufficient power generation or energy storage. Present strategies that curtail the renewable power generations of standalone dc micro grids if the battery bank cannot absorb the excess generation. These curtailment strategies restrict the batteries charging rate by the maximum absorbing power. Standalone dc micro grids are usually located in small-scale areas where the power sharing between DGs can be managed by centralized algorithms which are less affected by two issues:

a) Batteries in charging mode are nonlinear loads causing distortions to the grid voltage

b) The absolute voltage level of a standalone microgrid is shifted as the result of the load demand variation. A number of phenomena affect the batteries operation during the charging mode [19]:

- 1) Applying high charging currents, the batteries voltages quickly reach to the gassing threshold.
- 2) The internal resistor and hence power losses and thermal effects increase at high SOC levels.
- 3) Batteries cannot be fully charged with a constant high charging current.

Operational constraint, the maximum absorbed power by the batteries in order to protect them from being overcharged. Therefore batteries act as nonlinear loads during the charging mode. Depending on the proportion of the power generation to the load demand ratio within standalone DC microgrids, three cases are possible.

- 1) Power generation and load demand are balanced;
- 2) Load demand exceeds power generation causes dc bus voltage to drop in absence of any load shedding; and
- 3) Power generation is higher than load demand leads batteries to be overcharged and bus voltage to climb.

Energy management strategy (EMS) is proposed, as its control objectives, three aforementioned issues corresponding standalone dc micro grids; i.e., dc bus voltage regulation, proportional power sharing, and battery management. In contrast to the strategies available in literature in which renewable energy systems (RESs) always operate in their MPPT mode, the proposed multivariable strategy uses a wind turbine and a PV array as controllable generators and curtails their generations if it is necessary. The proposed EMS is developed as an online novel NMPC strategy that continuously solves an optimal control problem (OCP) and finds the optimum values of the pitch angle and three switching duty cycles.

It simultaneously controls four variables of micro grids:

- 1) Power coefficient of the wind turbine.
- 2) Angular velocity of the wind generator.
- 3) Operating voltage of the PV array and
- 4) Charging current of the battery bank.

It is shown that, employing new available nonlinear optimization techniques and tools, the computational time to solve the resulting NMPC strategy is in permissible range. The proposed strategy implements the IU charging regime that helps to increase the batteries life span.

## 2. Related Work

### 2.1 Block diagram:

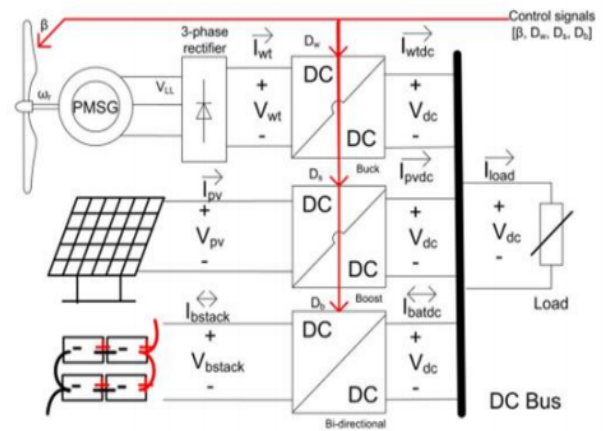


Fig. 1. Topology of a small-scale and standalone dc microgrid.

### DESCRIPTIONS:

The standalone dc micro grid in above figure is a smallscale microgram for remote applications. The wind turbine operates at variable speeds and is connected to the electrical generator directly, that is, the direct-drive coupling. The variable speed operation is more flexible for the power management and MPPT applications. Furthermore, direct-drive coupling is more efficient and reliable and is more popular for small-scale wind turbines. In spite of high cost, permanent magnet synchronous generators (PMSGs) are the most dominant type of direct-drive generators in the market, chiefly due to higher efficiency.

### 2.2 MODELING:

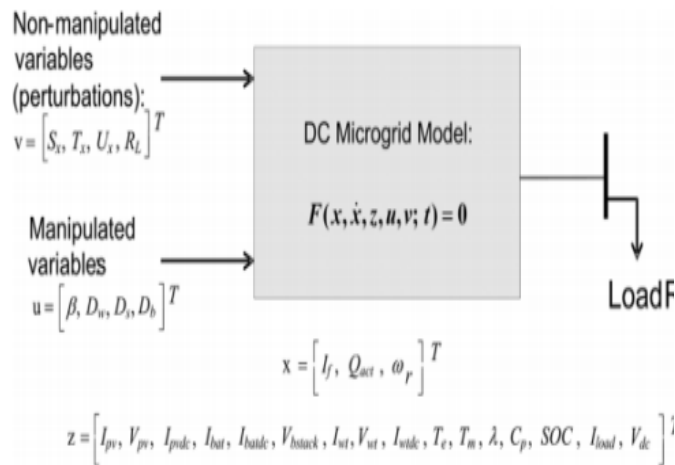


Fig2. Modified version of the system model.

The authors in [15] presented a mathematical model of standalone green dc microgrids as hybrid differential algebraic equations (hybrid DAEs). Fig. 2 summarizes a modified version of the proposed model in [2]. Since this paper focuses on the case in which there is an excess power greater than or equal to the maximum possible absorbing rate of the battery bank, the hybrid nature of the battery bank operation is ignored for the sake of simplicity. The differential and algebraic states, i.e., and, and the manipulated and nonmanipulated control variables, namely, and, are detailed later throughout the next sub-sections. In what follows, the following notations are used to model the standalone dc microgrid in Fig. 1 as DAEs:

$$\mathcal{F}(x, \dot{x}, z, u, v) = \begin{bmatrix} f_1(x, \dot{x}, z, u, v) \\ f_2(x, \dot{x}, z, u, v) \\ \dots \\ f_{24}(x, \dot{x}, z, u, v) \end{bmatrix} = 0 \quad (1)$$

The first two constraints  $f_1$  and  $f_2$  are due to the fact that in standalone dc microgrids the sum of the generated, stored, and consumed powers is always zero:

$$f_1 = V_{dc} (I_{pvdc} + I_{wt dc} + I_{batdc} - I_{load}), \quad (2a)$$

$$f_2 = V_{dc} - I_{load} R_L. \quad (2b)$$

### Modeling of the Three Systems:

#### A. Wind Branch.

#### B. Battery Branch.

#### C. Solar Branch.

#### A. Wind Branch

Performance of the wind turbines is measured as the power coefficient curve with respect to the tip speed ratio and pitch angle. Equation (3) shows the power coefficient curve of three-blade wind turbines:

$$f_3 = C_{p,norm} - \frac{1}{C_{p,max}} \times (C_1 \left( \frac{C_2}{\lambda_i} - C_3\beta - C_4 \right) \exp\left(-\frac{C_5}{\lambda_i}\right) + C_6\lambda), \quad (3)$$

$$f_4 = \lambda - \frac{Rad \times \omega_r}{U_x}, \quad (3)$$

$$f_5 = \lambda_i - \left( \frac{1}{\lambda + 0.08\beta} - \frac{0.035}{\beta^3 + 1} \right)^{-1}, \quad (3)$$

Where gamma and beta, respectively, are the tip speed ratio and pitch angle. Rad is the radius of the blades and Cp, max is the maximum achievable power coefficient at the optimum tip speed ratio of gamma out.

Equation (4) presents the connected PMSG generator:

$$f_6 = \frac{d\omega_r}{dt}(t) - \frac{1}{J}(T_e - T_m - F\omega_r), \quad (4a)$$

$$f_7 = -T_e \times \omega_r - I_{wt dc} \times V_{dc}, \quad (4b)$$

$$f_8 = -T_m \times \omega_r - \left( C_{p,norm} \left( \frac{U_x}{U_{x,base}} \right)^3 P_{nom} \right), \quad (4c)$$

Energy management strategies of microgrids must estimate the dc bus voltage level deviation from its set point in about every 5–10 s. It means that except the angular velocity of the generator (4a) all other fast voltage and current dynamics can be ignored. For energy management strategies, the average model of the buck converter is replaced with the steady-

state equations for the continuous conduction mode (CCM)

$$f_9 = V_{dc} - D_w V_{wt}, \quad (5a)$$

$$f_{10} = I_{wt} - D_w I_{wt dc} \quad (5b)$$

where Dw is the switching duty cycle of the converter and all remaining parameters are as depicted in Fig. 1. The average dc output voltage of the rectifier, Vwt, in presence of the non-instantaneous current commutation is calculated as follows.

$$V_{wt} = 1.35V_{LL} - \frac{3}{\pi} \omega_e L_s I_{wt} \quad (6)$$

$$f_{11} = I_{wt dc} - \frac{\pi}{3P\omega_r L_s D_w} \left\{ \frac{1.35\sqrt{3}P\psi\omega_r}{\sqrt{2}} - \frac{V_{dc}}{D_w} \right\}. \quad (7)$$

### B. Battery Branch:

Charging operation of a lead acid battery bank, consisting of (Nbatp\*Nbats) batteries, is modeled as:

$$f_{12} = \frac{V_{bstack}}{N_{bats}} - V_0 + R_{bat} \frac{I_{bstack}}{N_{batp}} + \frac{P_1 C_{max}}{C_{max} - Q_{act}} Q_{act} + \frac{P_1 C_{max}}{Q_{act} + 0.1 C_{max}} I_f, \quad (8)$$

$$f_{13} = \frac{dQ_{act}}{dt}(t) - \frac{1}{3600} \frac{I_{bstack}(t)}{N_{batp}}, \quad (8)$$

$$f_{14} = \frac{dI_f}{dt}(t) + \frac{1}{T_s} (I_f - \frac{I_{bstack}}{N_{batp}}), \quad (8)$$

$$f_{15} = V_{bstack} - \frac{V_{dc}}{1 - D_b}, \quad (8)$$

$$f_{16} = I_{bstack} - (1 - D_b) I_{batdc}, \quad (8)$$

$$f_{17} = SOC - \left\{ 1 - \frac{Q_{act}}{C_{max}} \right\} \quad (8)$$

the voltage, current, and state of charge of the battery bank. If is the filtered value of the battery current with the time constant of Ts and Qact is the actual battery capacity. The experimental parameter P1 requires being identified for each type of battery while the maximum amount of the battery capacity, Cmax, internal resistor of battery, Rbat, and the battery constant voltage, V0, are given by manufacturers. By ignoring the discharging mode of the battery bank operation, the bi-directional converter acts as a boost type converter [(8d)–(8e)].

### C. Solar Branch:

The equivalent electrical circuit of the PV module [7], [8] is used to mathematically model the solar branch, consisting of a PV array and a boost converter [9]. Eq. (9) shows the

characteristic equations of a PV array, consisting Npvp\*Npvs of PV modules:

$$f_{18} = I_{pv} - I_{ph} + I_0 \left\{ \exp\left(\frac{V_{pv} + \frac{N_{pvs}}{N_{pvp}} R_s I_{pv}}{n_d N_s} \frac{q}{KT_c} \times N_{pvs}\right) - 1 \right\} + \frac{V_{pv} + \frac{N_{pvs}}{N_{pvp}} R_s I_{pv}}{\frac{N_{pvs}}{N_{pvp}} R_{sh}}, \quad (9a)$$

$$f_{19} = I_{ph} - N_{pvp} \times \left( \frac{R_s + R_{sh}}{R_{sh}} I_{sc, stc} + k_I (T_c - T_{c, stc}) \right) \frac{S}{S_{stc}}, \quad (9b)$$

$$f_{20} = I_0 - N_{pvp} \times \frac{I_{sc, stc} + k_I (T_c - T_{c, stc})}{\exp\left(\frac{V_{oc, stc} + k_V (T_c - T_{c, stc})}{n_d N_s} \frac{q}{KT_c}\right) - 1} \quad (9c)$$

Where Iph denotes the photocurrent and I0 is the diode reverse saturation current. Rs and Rsh, respectively, are the series and parallel equivalent resistors of each PV module and all other parameters.

## 3. Implementation

### 3.1 CONTROLLER DESIGN:

#### Optimal Control Problems (OCPs):

OCPs, as (11), make explicit use of the system model, given by (11b), in order to find an optimal control law u\*(.), which meets number of equality and inequality constraints. The term optimal here is defined with respect to a certain criterion that implies the control objectives. This criterion is specified with a cost functional J, consisting of the Lagrangian term lambda and the terminal cost term M. While the Lagrangian term indicates the cost function during the

period of time, the terminal cost penalizes final values. Equations (11d) and (11e), respectively, formulate the final and initial constraints which must be maintained by the optimal solution. Moreover, (11g) represents boxing constraints on the states and control variables:

$$u^*(.) = \arg \underset{u(.) \in \mathbb{R}^n}{\text{minimize}} \quad J(x(t), z(t), u(t), T) :=$$

$$\int_t^{t+T} \mathcal{L}(x(\tau), z(\tau), u(\tau)) d\tau + \mathcal{M}(x(T), z(T)) \quad (11a)$$

$$\text{s.t.: } \mathcal{F}(x(t), \dot{x}(\tau), z(\tau), u(\tau), v(\tau)) = 0 \quad (11b)$$

$$\mathcal{H}(x(\tau), z(\tau), u(\tau)) \leq 0 \quad (11c)$$

$$\mathcal{R}(x(T), z(T)) = 0 \quad (11d)$$

$$x(\tau) = x_0, z(\tau) = z_0 \quad (11e)$$

$$\forall \tau \in [t, t+T] \quad (11f)$$

$$x(\tau) \in \mathcal{X}, z(\tau) \in \mathcal{Z}, u(\tau) \in \mathcal{U}. \quad (11g)$$

### Nonlinear Model Predictive Control (NMPC):

OCPs are open-loop strategies and are wrapped by a feedback loop to construct NMPC strategies [10]. NMPC strategies, which are also called as the receding horizon control, continuously solve an OCP over a finite-horizon T using the measurements obtained at t as the initial values. Then the first optimal value is applied as the next control signal.

Comparing with the conventional methods, NMPCs are inherently nonlinear and multivariable strategies that handle constraints

and delays. There are three different techniques to discretize and solve OCPs:

- 1) Dynamic programming method based on the Bellman's optimality principle.
- 2) Indirect method based on the Pontryagin minimum principle.
- 3) Direct methods that convert OCPs into nonlinear optimization problems (NLPs) which are then solved by NLP solvers.

### Control System:

Since it focuses on the charging mode of the battery operation, the proposed EMS successively gets the estimated system states, as inputs and calculates the optimal solution, as outputs. The external state estimator and the predictor of the non-manipulated variables are out of the scope of this paper. Step ahead predictions of the solar irradiance, wind speeds, and load demands are extracted either from a meteorological center or an external predictor using autoregressive-moving-average (ARMA) technique [7]. The bus voltage level of the microgrid is set externally and hence the developed controller can act as the secondary and primary levels of the hierarchical architecture [13].

The developed NMPC controller consists of three entities:

- 1) The dynamic optimizer that successively solves OCP at each sampling time h,

- 2) The mathematical model of the system to predict its behavior
- 3) The cost function and constraints of the relevant OCP.

The optimal pitch angle is applied as a set point to an inner closed-loop controller. Moreover, the optimal values of the switching duty cycles are applied to the pulse width modulators (PWMs) of the dc-dc converters.

## 4. Experimental Work

### 4.1 Simulation circuit design in Matlab:

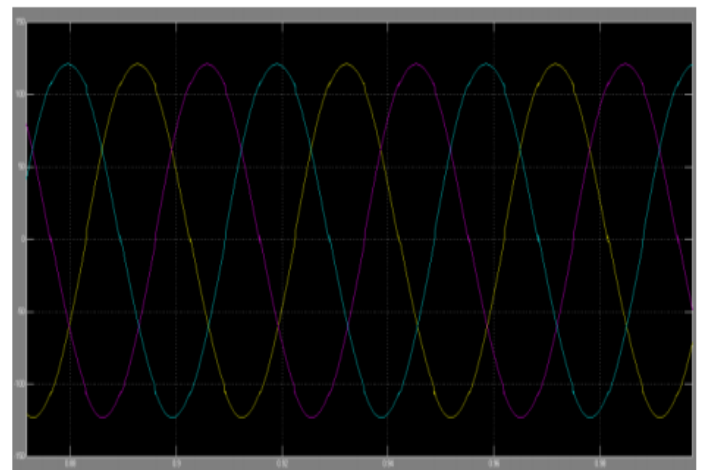
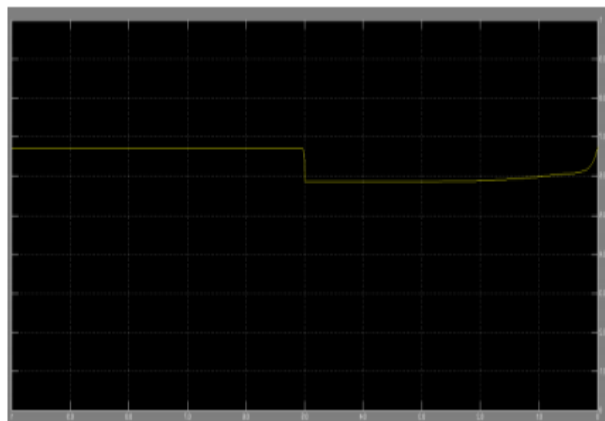
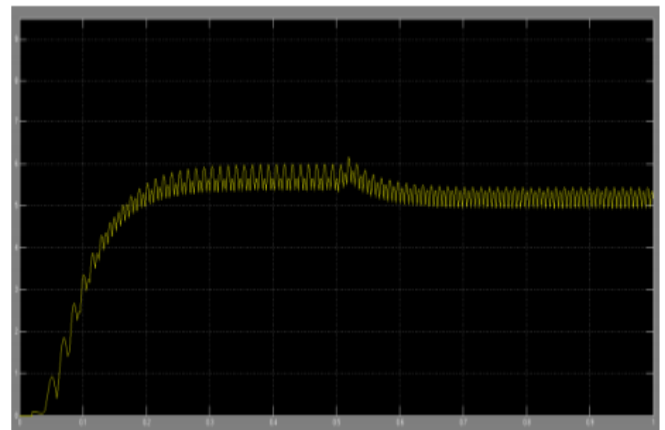
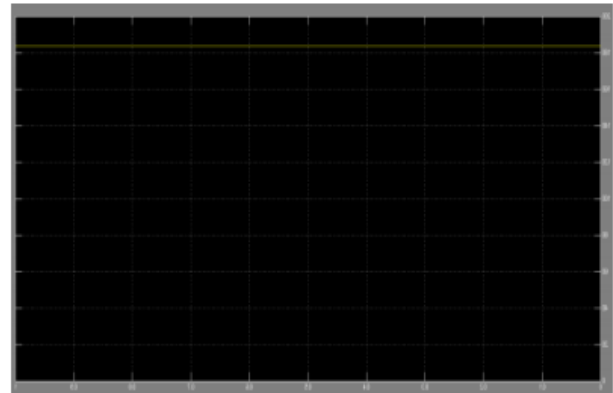
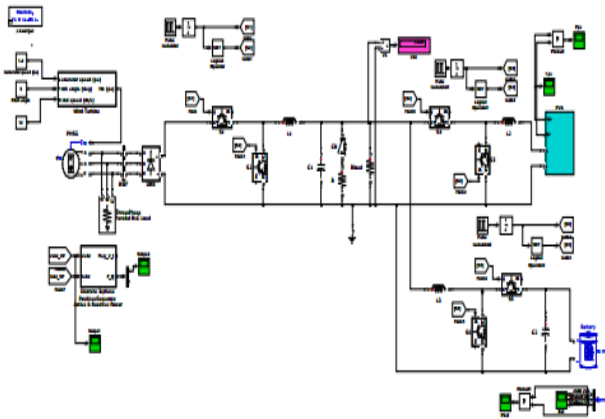


Fig shown: Output wave forms of the simulation.

## 5. Conclusion



A coordinated and multivariable online NMPC strategy has been developed to address the optimal EMS, which deals with three main control objectives of standalone dc microgrids. These objectives are the voltage level regulation, proportional power sharing, and battery management. In order to address these objectives, the developed EMS simultaneously controls the pitch angle of the wind turbine and the switching duty cycles of three dc/dc converters. It has been shown that the developed controller tracks the MPPs of the wind and solar branches within the normal conditions and curtails their generations during the under load conditions. The provided flexible generation curtailment strategy realizes the constant current, constant voltage charging regime that potentially increases the life span of the battery bank. The simulation results have been shown its ability to achieve all control objectives.

## 6. References

- [1] Arash M. Dizqah, Alireza Maheri, Krishna Busawon, and Azadeh Kamjoo “A Multivariable Optimal Energy Management Strategy for Standalone DC Microgrids,” IEEE transactions on power systems, vol. 30, no. 5, pp 2278-2287, September 2015.
- [2] R. S. Balog, W. W. Weaver, and P. T. Krein, “The load as an energy asset in a distributed DC smartgrid architecture,” IEEE Trans. Smart Grid, vol. 3, no. 1, pp. 253–260, 2012.
- [3] J. M. Guerrero, M. Chandorkar, T. Lee, and P. C. Loh, “Advanced Control Architectures for Intelligent Microgrids-Part I: Decentralized and Hierarchical Control,” IEEE Trans. Ind. Electron., vol. 60, no. 4, pp. 1254–1262, 2013.
- [4] S. An and, B. G. Fernandes, and M. Guerrero, “Distributed control to ensure proportional load sharing and improve voltage regulation in low-voltage DC microgrids,” IEEE Trans. Power Electro., vol. 28, no. 4, pp. 1900–1913, 2013.
- [5] Chen and L. CSU, “Autonomous DC voltage control of a DC microgrid with multiple slack terminals,” IEEE Trans. Power Syst., vol. 27, no. 4, pp. 1897–1905, Nov. 2012.
- [6] Zhao, X. Zhang, J. Chen, C. Wang, and L. Guo, “Operation optimization of standalone microgrids considering lifetime characteristics of battery energy storage system,” IEEE Trans. Sustain. Energy, Volume: 4, n0.4, pp: 934 - 943 Oct. 2013.
- [7] J. M. Guerrero, J. C. Vasquez, J. Matas, L. G. de Vicua, and M. Castilla, “Hierarchical control of droop-controlled AC and DC microgrids-a general approach toward standardization,” IEEE Trans. Ind. Electron., vol. 58, no. 1, pp. 158–172, 2011.

- [8] P. H. Divshali, A. Alimardani, S. H. Hosseinian, and M. Abedi, "De-centralized cooperative control strategy of microsources for stabilizing autonomous VSC-Based microgrids," *IEEE Trans. Power Syst.*, vol. 27, no. 4, pp. 1949–1959, Nov. 2012.
- [9] H. Fakham, D. Lu, and B. Francois, "Power control design of a battery charger in a hybrid active PV generator for load-following applications," *IEEE Trans. Ind. Electron.*, vol. 58, no. 1, pp. 85–94, 2011.
- [10] X. Liu, P. Wang, and P. C. Loh, "A hybrid AC/DC microgrid and its co-ordination control," *IEEE Trans. Smart Grid*, vol. 2, no. 2, pp. 278–286, 2011.
- [11] Meharrar, M. Tioursi, M. Hatti, and A. B. Stambouli, "A variable speed wind generator maximum power tracking based on adaptative neuro-fuzzy inference system," *Expert Syst. Applicat.*, vol. 38, no. 6, pp. 7659–7664, 2011.
- [12] O. Tremblay and L. Dessaint, "Experimental validation of a battery dynamic model for EV applications," *World Elect. Vehicle Journal.*, vol. 3, pp. 10–15, 2009.
- [13] M. Dizqah, K. Busawon, and P. Fritzson, "Acausal modeling and simulation of the standalone solar power systems as hybrid DAEs," in *Proc. 53rd Int. Conf. Scandinavian Simul. Soc.*, 2012.
- [14] N. Mohan, T. M. Undeland, and W. P. Robbins, *Power Electronics: Converters, Applications, and Design*. New York, NY, USA: Wiley, 1995.
- [15] J. H. Su, J. J. Chen, and D. S. Wu, "Learning Feedback Controller Design of Switching Converters Via MATLABSIMULINK," *IEEE Transactions on Education*, vol. 45, pp. 307–315, 2002.
- [16] L. Grüne and J. Pannek, "Nonlinear model predictive control: Theory and algorithms," in *Communications and Control Engineering*. New York, NY, USA: Springer, 2011.
- [17] R. Neidinger, "Introduction to automatic differentiation and MATLAB object-oriented programming," *SIAM Rev.*, vol. 52, no. 3, pp. 545–563, 2010.